Arabian Journal of Chemistry (2022) **15**, 103572

King Saud University

Arabian Journal of Chemistry

www.ksu.edu.sa
www.sciencedirect.com

ORIGINAL ARTICLE

Therapeutic effect of two Co(II) coordination polymers by inhibiting tumor cell proliferation and invasion on pancreatic cancer

Fa-Zhao Li [a], Jun He [b], Su-Shun Liu [b], Le-Ping Yang [b,*], Dong Xue [c]

[a] *Liver and Gallbladder Surgery Ward, the Second Xiangya Hospital of Central South University, Changsha, Hunan, China*
[b] *Pancreatic and Gallbladder Surgery Ward, the Second Xiangya Hospital of Central South University, Changsha, Hunan, China*
[c] *Department of Medicine, Henan University of Science and Technology, Luoyang, Henan, China*

Received 26 September 2021; accepted 14 November 2021
Available online 17 November 2021

KEYWORDS

Coordination polymers;
Co complex;
CCK-8 assay;
Pancreatic cancer;
Molecular docking

Abstract In this work, through utilizing the mixed-ligand synthesis method, two coordination polymers (CPs) based on Co(II), namely, $\{[Co(\mu\text{-ppda})(\mu\text{-pbmeix})]\cdot H_2O\}_n$ (**2**) and $[Co(\mu\text{-opda})(\mu\text{-pbmeix})_{0.5}]_n$ (**1**) have been triumphantly formed from 1,4-bis(2-methylimidazol-1-ylmethyl)benzene (pbmeix), a semi-rigid ligand with Co(II) nitrate salts and distinct carboxylic acid co-ligands (o/p-H$_2$pda = 1,2-/1,4-phenylenediacetate). For treatment of pancreatic cancer, the as-generated compounds' inhibitory activity against the viability of cancer cell was determined by the Cell Counting Kit-8 (CCK-8) assay. The above compounds' suppression effect against the cells invasion and migration activity was investigated by the trans-well detection. The real time reverse transcription-polymerase chain reaction (RT-PCR) subsequently was employed to test the VEGF signaling pathway activation. Eventually, the cancer cells apoptosis levels after treating with above compound were assessed via detecting the BCL-2 protein expression level. Furthermore, results from molecular docking simulation indicate that complex **1** not only exhibits relatively lower affinity energy, but also forms more binding interactions in comparison to complex **2** when binding to a given target protein. Complex **1** was much superior to complex **2** on treating pancreatic cancer via suppressing the cancer cell invasion, migration and viability ability.

1. Introduction

Pancreatic cancer is one of the most malignant tumors of the digestive tract. It progresses quickly, has a poor prognosis, is easy to relapse, and has a short survival period (Tempero, 2019). The survival rate within five years is less than 5%. Its fatality rate ranks eighth in the world. At present, the molecular regulation mechanism for the invasion together with metas-

* Corresponding author.
E-mail address: 502257@csu.edu.cn (L.-P. Yang).
Peer review under responsibility of King Saud University.

Production and hosting by Elsevier

https://doi.org/10.1016/j.arabjc.2021.103572
1878-5352

tasis of the pancreatic cancer is not fully understood (Bear et al., 2020). Therefore, exploring the above mechanism of the invasion together with metastasis of the pancreatic cancer may provide an experimental basis for the development of new molecular targeted therapies for the treatment of pancreatic cancer (Ansari et al., 2016).

In recent years, the reasonable design of CPs-based functional materials has received widespread attention, on account of their fascinating topologies and architectural diversities, at the same time because of their applications in fluorescence, separation, gas capture, drug delivery, fluorescence sensing, proton conductivity as well as other associated fields (Pan et al., 2020; Liu et al., 2021; Liu et al., 2021; Dutta et al., 2021). The generation of ideal CPs having useful performances is affected via some key factors, for example the types of functional motif of ligands, template, concentration, auxiliary ligand, solvent system, temperature, pH and the time of reaction. Many studies have been devoted to the establishment of CPs by the combination of N-donor ligands and carboxylic acids (Karadagi et al., 2020; Rashidi et al., 2020; Abedi et al., 2019; Aghaee et al., 2021; Souri et al., 2018; Pepió et al., 2021; Zhong et al., 2020; Wang et al., 2012). On the other hand, Cobalt as a human essential element in the active site of vitamin B12, which indirectly regulates the synthesis of DNA, has attracted many biological and organometallic chemists who have investigated cobalt complexes with the aim of medical applications, due to their significant bioactivity. According to the literature, cobalt complexes have been shown to possess antibacterial, antifungal, antiviral, antiparasitic and antioxidant activity, and antitumor and antiproliferative activity (Sukanya and Reddy, 2018; Zhang et al., 2016; Lei et al., 2018; Jagadeesan et al., 2013). In experimental investigation of malignant tumor therapy, the interest in cobalt complexes results from their role as systemic anticancer agents as well as their ability to redox-dependent target the malignant tissue of solid tumors. Many cobalt complexes having anticancer activity have been reported. For example, Raja et al. synthesized a cobalt(II) coordination polymer of isonicotinic hydrazine with substantial anticancer activity (Raja et al., 2012). In this work, through utilizing the mixed-ligand generation method, two fresh CPs based on Co(II), namely, {[Co(μ-ppda)(μ-pbmeix)]·H_2O}$_n$ (**2**) and [Co(μ-opda)(μ-pbmeix)$_{0.5}$]$_n$ (**1**), have been triumphantly formed from 1,4-bis(2-methylimidazol-1-ylmethyl)benzene (pbmeix), a semi-rigid ligand with Co(II) nitrate salts and distinct carboxylic acid co-ligands (o/ppda = 1,2-/1,4-phenylenediacetic acid). The as-created two coordination polymers have been investigated through the diffraction of single crystal X-ray, EA, PXRD, TGA and FT-IR. In the bio-section, the above two compounds' treatment activity against the pancreatic cancer was examined. From the molecular and structural points of view, although a slightly change in the Co complex structure has been applied during the synthesis, the functionality of the complex may vary in a large range, thus, in addition to the experiment, the simulation of molecular docking has been implemented for investigating the difference between the two synthesized Co complex and for understanding the capability of the anti-cancer effect. Thus, we confirmed that complex **1** was much superior to complex **2** on treating pancreatic cancer via suppressing the cancer cell invasion, migration and viability ability.

2. Experimental

2.1. Chemicals and measurements

In this paper, the solvents and chemicals applied were provided by commercial sources with the reagent quality and they can be utilized directly. With the aim of investigating the elements of Carbon, Nitrogen together with Hydrogen, Perkin-Elmer model 240C was employed. Bruker D8 Advance X-Ray diffractometer was applied to conduct the detection of PXRD utilizing 0.15418 nm Cu Kα radiation, where the X-Ray tube worked at 30 mA and 40 kV. With the temperature between RT and 800 °C, by utilizing Perkin Elmer, TGA was implemented at 20 K per min increasing rate with N_2 flow. The spectrophotometer of Nicolet (Impact 410) was employed to determine the compounds' IR absorption spectra between 400 and 4000 cm^{-1} utilizing KBr pellets.

2.2. Preparation and characterization for [Co(μ-opda)(μ-pbmeix)$_{0.5}$]$_n$ (1)

The mixture synthesized from 0.15 g and 0.8 mmol H_2opda, 0.1 mmol and 30 mg $Co(NO_3)2{\cdot\cdot}6H_2O$ and 0.21 g and 0.8 mmol pbmeix was lysed in a 32 mL solution of H_2O and DMF (with the volume ratio of 3:1) in a Parr acid digestion bomb (45 mL) lined by teflon. The above mixture was maintained and next heated for seven days under a temperature of 120 °C, prior to cooling with 5 °C·h^{-1} rate to RT. Eventually, the compound 1's pink crystals were gathered via filtration and cleaned through water. Anal. Calcd for $C_{18}H_{17}CoN_2O_4$: C, 56.26; H, 4.46; N, 7.29%. Found: C, 56.85%; H, 4.29%; N, 7.54%. FTIR (KBr, cm^{-1}, Fig S1): 723 m, 1153w, 1271 m, 1367 s, 1411 s, 1440 s, 1552 vs, 1631 s, 2914w, 2960w, 3026w, 3059w, 3128 w.

2.3. Preparation and characterization for {[Co(μ-ppda)(μ-pbmeix)]·H_2O}$_n$ (2)

The mixture formed by 0.10 g and 0.5 mmol H_2ppda, 0.1 mmol and 30 mg $Co(NO_3)2{\cdot\cdot}6H_2O$ and 0.14 g and 0.5 mmol pbmeix was lysed in a 12 mL solution of H_2O and DMF (with the volume ratio of 3:1) in thick walled glass tube. The above mixture was kept and next heated for three days under a temperature of 120 °C, prior to cooling with 5 °C·h^{-1} rate to RT. Filter the solution and allow it to evaporate slowly. After several days, the **2**'s colourless crystals were gathered via filtration and cleaned through applying water. Anal. Calcd for $C_{26}H_{28}CoN_4O_5$: C, 58.32; H, 5.27; N, 10.46%. Found: C, 58.27%; H, 5.69%; N, 10.87%. FTIR (KBr, cm^{-1}): 740m, 1144w, 1277m, 1364s, 1422s, 1440s, 1516 vs, 1602s, 1606s, 2914w, 2963w, 3000w, 3130w, 3510w.

The diffractometer of SuperNova was employed with the aim of gaining the X-Ray data. CrysAlisPro was applied for the exploration of the strength data, which was subsequently converted to the HKL files. The direct mean based-SHELXS together with the least-squares method based SHELXL-2014 software were respectively employed to synthesize and modify the original architectural modes (Sheldrick, 2015). The anisotropic parameters were mixed after using the whole non-H

atoms. Eventually, the entire H-atoms could be fixed on the C atoms that they are linked to in geometry with AFIX commands. The complexes' optimization details together with their parameters of crystallography were listed in the Table 1. The selected bond lengths and angles are listed in Tables S1-S4 in the ESI.

2.4. CCK-8 assay

In this experiment, the CCK-8 assay was implemented to determine the compounds' inhibitory activity against the viability of pancreatic cancer. This conduction was performed strictly following the instructions accompanied with some modifications. Shortly, the pancreatic cancer cells of PC-1 (obtained from ATCC) in logical growth were gathered and then inoculated into the plates (96 well, 10^4 cells /well). The cells were stored in a 37 °C incubator, with 5% CO_2 for half a day. After incubation for twelve hours, the wells were added with the compounds with various concentrations (between 0 and 80 μM). Subsequently, discarding the medium of cell culture and adding the fresh medium involving CCK-8 reagent (10 μL) into the wells. After finishing the specific treatment, for each well, the absorbance was tested at 490 mm. This study was implemented for 3 times or more, and the results were described with mean ± SD.

2.5. Trans-well assay

In order to in-depth measure the invasion and migration ability of the pancreatic cancer cells of PC-1 after treating with the above compound, in this study, the trans-well assay was carried out. The 24-well trans-well chambers were maintained in the plates (24-well), and in logical growth, the pancreatic cancer cells of PC-1 were inoculated into upper chambers and cultured in a fresh FBS medium. The complement couture medium was addressed into lower chambers. After incubation for one day under a temperature of 37 °C, with 5% CO_2, on upper membrane, the residual cells were removed, and the pancreatic cancer cells of PC-1 on the other cambers side were stained through utilizing the crystal violet (0.5%). On the lower membrane surface, the cells after stained were quantified through employing the microscope. All the implementation were carried out for the detection of cell migration. For the invasion test, the trans-well chamb[illegible]well) were pre-coated via the matrigel matrix ([illegible] Bioscien[illegible], NJ, USA), the subsequent protocols were im[illegible]duced as mer[illegible]oned above. This study was implemente[illegible] for [illegible]imes or m[illegible]re, and the results were described wit[illegible]ean ± S[illegible]

Table 1 The complexes' optimization details [illegible]gethe[illegible]with their parameters of crystallography.

Identification code	1	2
Empirical formula	$C_{18}H_{17}CoN_2O_4$	$C_{26}H_{28}$ [illegible] N_4O_5
Formula weight	384.26	535.45
Temperature/K	293(2)	293(2)
Crystal system	monocli[illegible]c	[illegible]linic
Space group	$P2_1$[illegible]	$P\bar{1}$
a/Å	12[illegible]638(11)	9.14260(13)
b/Å	1[illegible]712(1[illegible]	10.5529(2)
c/Å	9.16[illegible]	12.3725(4)
α/°	[illegible]00	85.263(3)
β/°	[illegible]00.5290([illegible]	73.0258(17)
γ/°	[illegible]00	88.5741(11)
Volume/Å^3	1678.[illegible]	1137.81(4)
Z	4	2
ρ_{calc}g/cm^3	1.528	1.563
μ/mm^{-1}	[illegible].053	6.322
Data/restraints/parameters	3520/0/227	4774/0/306
Goodness-of-fit on F^2	1.149	1.106
Final R indexes [I >= 2σ (I)]	R_1[a] = 0.0588, ωR$_2$ = 0.1363	R_1^b = 0.0828, ωR$_2$ = 0.2234
Final R indexes [all data]	R_1 = 0.0735, ωR$_2$ = 0.1460	R_1 = 0.0877, ωR$_2$ = 0.2323
Largest diff. peak/hole / e Å^{-3}	0.41/-0.45	1.89/-1.07
CCDC	2,111,923	2,111,924

[a] $R_1 = \Sigma||F_o| - |F_c||/\Sigma|F_o|$. [b] $wR_2 = |\Sigma w(|F_o|^2 - |F_c|^2)|/\Sigma|w(F_o)^2|^{1/2}$, where $w = 1/[2(F_o^2) + (aP)^2 + bP]$. $P = (F_o^2 + 2F_c^2)/3$.

2.6. Real time RT-PC[illegible]

The real time [illegible]-PCR was [illegible]om[illegible]shed for the detection of the VEGF [illegible]gnali[illegible] pathway ac[illegible]vation in the pancreatic cancer cells of PC-1 afte[illegible]reating via the above compounds. This imple[illegible]tion was ca[illegible]d out totally adhere to the instructio[illegible]. In brief, in logical growth, the pancreatic cancer cells of[illegible]C-1 were g[illegible]hered and then inoculated into the plates (6 we[illegible] with 10^6 c[illegible]s per well ultimate destiny). The cells were mai[illegible]ined in [illegible]37 °C incubator, with 5 %CO_2 for twelve hours, t[illegible]eatment was then finished with the above com[illegible]ds at specific concentrations. The cells were subsequently [illegible]athered, in the cells, the overall RNA could be extracted applying TRIZOL. After testing the overall RNA concentration, it was reverse transcripted subsequently into the cDNA. The VEGF signaling pathway relative expression in the pancreatic cancer cells of PC-1 was examined through exploiting real time RT-PCR, where *gapdh* was utilized as an internal control gene. The sequence of the *vegf* primers used in this research: CGAAAGCGCAAGAAATCCCG, GCTCCAGGGCATTAGACAGC. This study was implemented for 3 times or more, and the results were described with mean ± SD.

2.7. Western blotting assay

After treated by the synthesized compounds, the Bcl-2 protein expression levels in the pancreatic cancer cells of PC-1 were tested through using the western blotting assay. All the conduction in our paper was finished completely on the basis of the protocols with slight modifications. Briefly, in logical growth, the pancreatic cancer cells of PC-1 were gathered and then inoculated into the plates (6 well) with 10^5 cells per well destiny. After incubated at a 37 °C incubator, with 5 % CO_2 for twelve hours, the two compounds were utilized to treat cells with 50 ng/ml concentration. Applying 5-Fu as a positive control. After conducting the above treatment, we can extract the overall protein samples, and then determined its concentration by BCA Protein Assay Kit. The samples were subsequently isolated via the gel electrophoresis of SDS-PAGE and transferred into a PVDF membrane (0.22 mm) by electrophoresis. After incubated through applying the primary

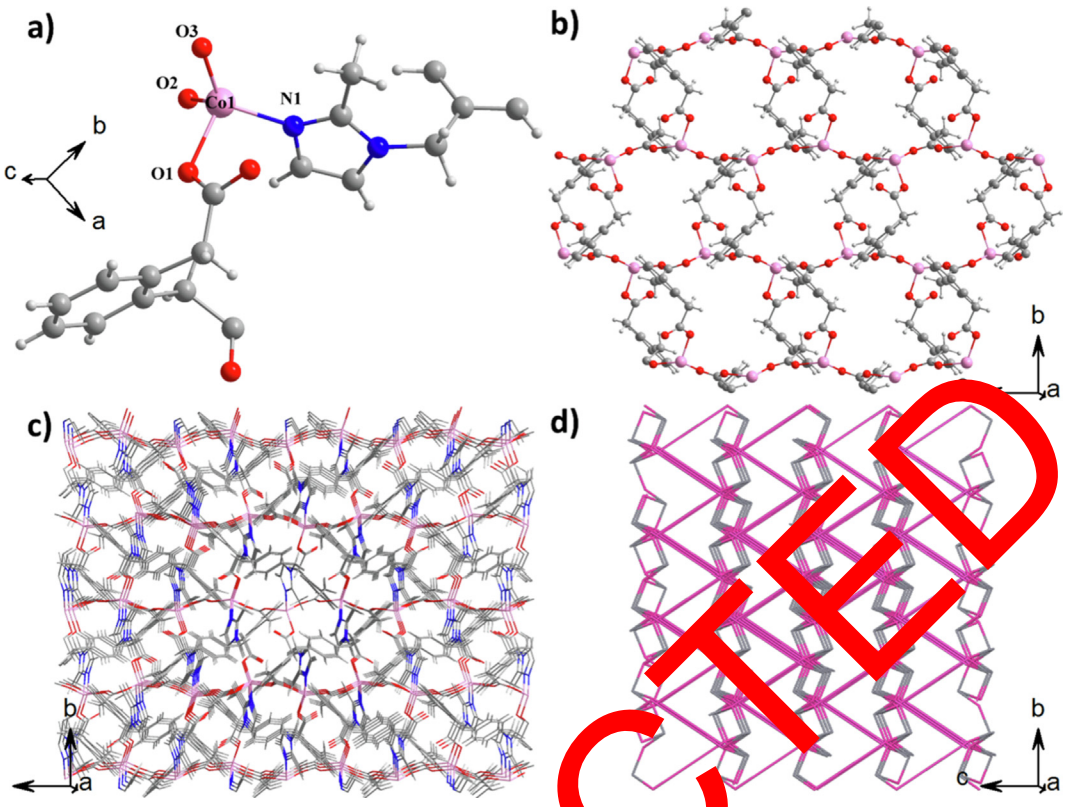

Fig. 1 (a) The coordination environments for the Co ion. (b) The 1′s 2-dimensional Co-opda layer. (c) The 3-dimensional framework of the compound 1. (d) The compound 1′s xww-3,4-P21/c top

antibody and suitable secondary antibody combined with the horseradish peroxidase, the images of protein could be captured. This study was implemented for 3 times of the results were described with mean ± SD.

2.8. Simulation details

In order to feed the Co complexes into the molecular docking simulation, the two synthesized Co complexes, namely, complexes **1** and **2**, have been constructed by Avogadro 1.2 and default energy minimization has been applied. Regarding the target protein, the VEGF protein family has been chosen as the target protein reservoir, since the regulation of VEGF protein has been viewed as strong signaling probe for antitumor drug targets. Therefore, we choose 5 K65 from the VEGF protein family as the target protein since it contains a large docking pocket which is extremely suitable for capturing large size ligand (Lobner et al., 2017). The grid box that contains the docking pocket is located at the position of X = -17.511, Y = -24.087, Z = 23.164 (Å). In each direction, the number of grid points is 60, again, such number ensures that the gird box is big enough for allowing the Co complex to adjust their conformations during the docking simulation. For both Co complexes, 9 rotatable dihedrals have been found, thus, under the better sampling consideration, 50 binding poses have been adopted with the Lamarckian genetic algorithm (LGA). All the simulations have been performed by AutoDock 4.2 and AutoDockTools 1.5.6.

3. Results and discussion

3.1. Crystallography description

Compound **1** was generated with the reaction between Co(II) acetate and pbmeix and H_2opda in a solution of water and DMF at 120 °C. The compound was crystallised in a monoclinic *P*21/*c* space group and its fundamental unit involves a Co(II) centre, a opda and 0.5 pbmeix (Fig. 1a). The center of Co(II) is 4-coordinated, combining with three O atoms belong to three distinct opda and a N atom provides by a pbmeix. It reveals twisted tetrahedral structure (where τ_4 is equal to 0.81), and the angles of bond is between 98.08(12) and 127.32(18)°. The bond lengths of Co(1)–O ranging from 1.916(3) to 0.019 (2) Å and the bond distance of Co(1)–N(1) is 1.990(3) Å. The carboxylic acid group involving O(1) and O(2) connects between the centres of Co(II), resulting in the creation of chains along axis *c* in crystallography. These chains are linked into sheets through opda connectors. On the whole, the opda connectors utilize the μ_3-κ^1: κ^1: κ^1: κ^0 coordination manner via connecting the centres of Co(II), and opda employ the trans conformation and creates sheets on plane *bc* (Fig. 1b). The length between the centres of Co(II) linked via the pbmeix connector is 14.303 Å. The torsion angles between carboxylic acid groups and the neighboring aromatic rings through C1–C2–C3–C4 and C10–C9–C8–C7 respectively are –98.64° and –103.02°. The neighboring sheets are inter-connected through pbmeix to synthesize a 3-dimensional skeleton (Fig. 1c). The

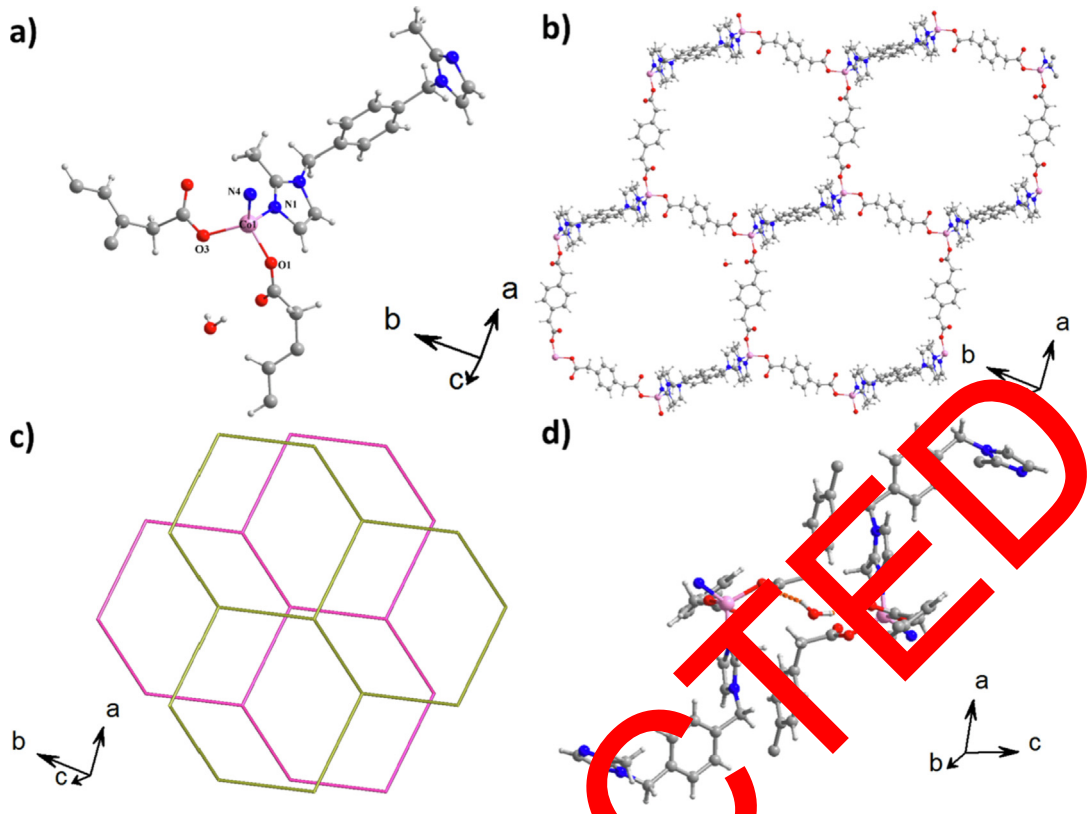

Fig. 2 (a) The coordination manner for the Co ions. (b) View 2-dimen[illegible]nal layer. (c) The parallel interpenetrated architecture of 2D + 2D → 2D. (d) The interactions of H-bond between the [illegible]boring layer.

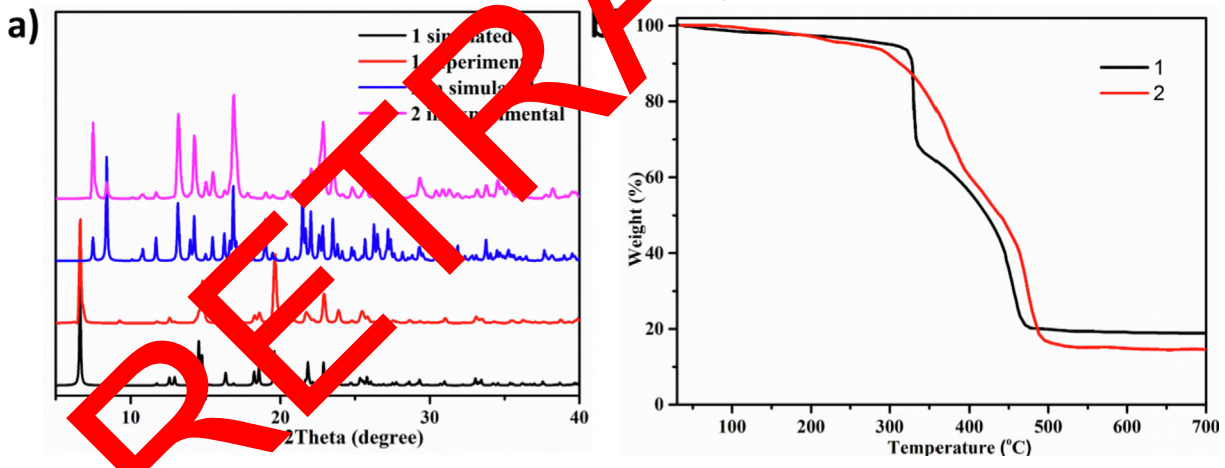

Fig. 3 (a) The patterns of PXRD for compounds 1 and 2. (b) and their curves of TGA.

analysis of topology exhibits that the **1** possesses a **xww**-3,4-*P*21/*c* topology with $(4.8^2 0.10^3)(4.8^2)$ point symbol (Fig. 1d).

Compound **2** was produced by the reaction between Co(II) acetate and pbmeix and H_2ppda in a solution of water and DMF at 120 °C. It was crystallized in a triclinic *P*–1 space group, and the **2**′s fundamental unit is constructed from a centre of Co(II), two half ligands of ppda, a pbmeix and a molecule included H_2O. According to Fig. 2a, the centre of Co(II) is coordinated via two O atoms of carboxylic acid groups come from two diverse ppda and two N atoms provided via two distinct pbmeix. It reveals twisted tetrahedral structure (where τ_4 is equal to 0.92), and the angles of bond is between 102.88 (12) and 115.69(12)°. The bond lengths of Co(1)–O(1), Co(1)–O(3), Co(1)–N(1) together with Co(1)–N(4) are 1.938(3), 1.945(2), 1.993(4) and 2.048 (4) Å. In comparison with complex **1**, there exist no linking carboxylic acid groups in compound **2**. The ppda ligand coordinates with metal centre using a μ_2-κ^1:κ^0:κ^1:κ^0 coordination manner, and the CH_2CO_2 groups twist each other in a classic trans conformation. Each ppda bridges two centres of Co(II) to produce an infinite 1D

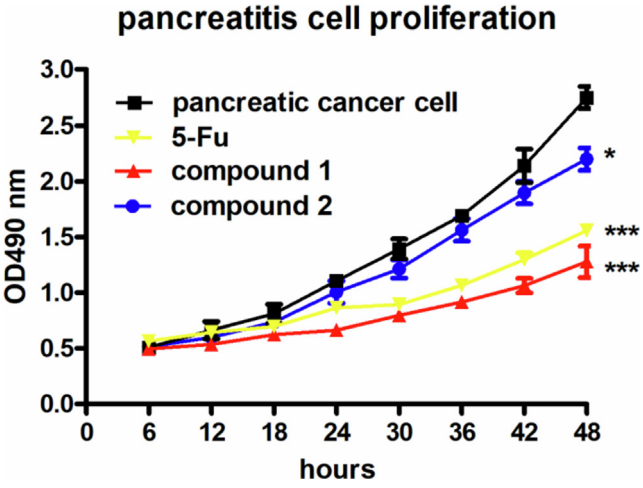

Fig. 4 Inhibition of the new compounds on the viability of PC-1 pancreatic cancer cells. In logical growth, the pancreatic cancer cells of PC-1 were gathered and inoculated into the plate of cell culture, the treatment was subsequently finished with the above compounds at various dilutions. The PC-1 pancreatic cancer cells viability was examined through the assay of CCK-8. * means $P < 0.05$ and *** means $P < 0.005$.

zig-zag polymeric chain, and consecutive chains are in-depth connected together through two diverse pbmeix to create a 2-dimensional net on plane *ab* (Fig. 2b). These sheets consist of large hexagonal rings (passing through a distan[illegible] of 17.8 Å). Four sides are composed of ppda, and two side[illegible] are composed of paired pbmeix, which themselves form the C[illegible]-pbmeix)$_2$ rings. The length between the centres of Co(II) co[illegible]nected via the pbmeix connectors is 11.667 Å in co[illegible]parison of complex **1** which shows 3D framewor[illegible] structu[illegible], the 2-dimensional layers of **2** penetrate each other to produce a parallel interpenetrated architecture of 2D + 2D → 2D (Fig. 2c). When ppda from a net penetrate $Co_2(pbmeix)_2$ rings of a consecutive networks, interpenetration appears, resulting in a polyketene architecture. The interlayers are in-depth extended into a 3-dimensional supramolecular net through the interactions of H-bond between coordinated H_2O molecules and carboxylic acid groups (Fig. 2d).

3.2. PXRD and TGA

For the sake of examining the phase purity for the products, the research of PXRD on the compounds created was accomplished (Fig. 3a). There exist a w[illegible] con[illegible]ency between the peak positions of PXRD patter[illegible] of experim[illegible]t and the simulation, and this funding exhibi[illegible] that the cry[illegible]l architecture really represents the prod[illegible]s of i[illegible]sive cryst[illegible]. The strength differences may be cau[illegible]d via crystal[illegible] impl[illegible] preferred selection. In order to in[illegible]stigate [illegible]e above [illegible]mpounds' thermal stabilities, the TGA w[illegible]e ac[illegible]mplished under air flow between 30 and 700 °C [illegible] the co[illegible]ounds. F[illegible] the **1**, there exist no significantly w[illegible]htlessness w[illegible]n th[illegible] temperature less than 263 °C, sugg[illegible]ing t[illegible]re are no c[illegible]ordinated or lattice solvents in the complex **1** and[illegible]his is in accordance with the outcomes in the[illegible]tion of crys[illegible] architecture. After the in-depth heat[illegible]g, a sharp weightlessness could be found on account of the [illegible]ecomposition[illegible] of the whole organic ligand. The final product [illegible]ove the tem[illegible]erature of 500 °C was CoO, (found: 19.41%, ca[illegible]: 19.27% [illegible]or **1**). For the **2**, the first weightlessness between 72 and [illegible]°C was associated with removal of the molecules [illegible]luded H_2O (with the found and calculated values of 3.18 % and 3.36% for complete **2**). On the in-depth heating, it was completely decomposed, and the residues is CoO (with a found and calculated value of 14.56% and 13.83% for **2**).

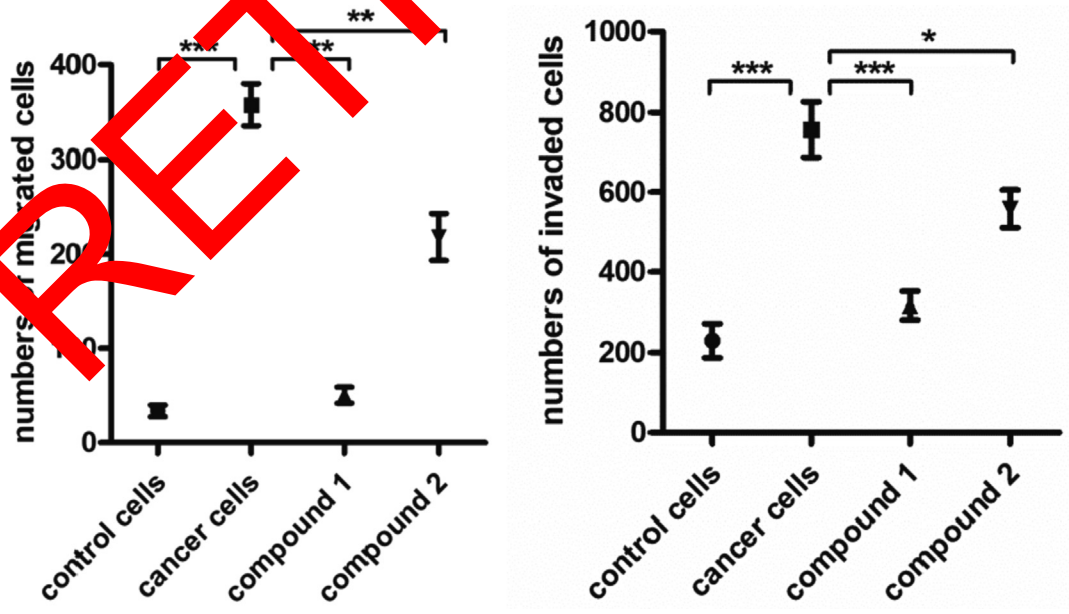

Fig. 5 Decreased invasion and migration of cancer cells after treated with the compound. The pancreatic cancer cells of PC-1 were inoculated into the plates (24 well), and then treating with above compounds. The trans-well detection was implemented and the invasion and migration ability for cancer cells were determined. * means $P < 0.05$ and *** means $P < 0.005$.

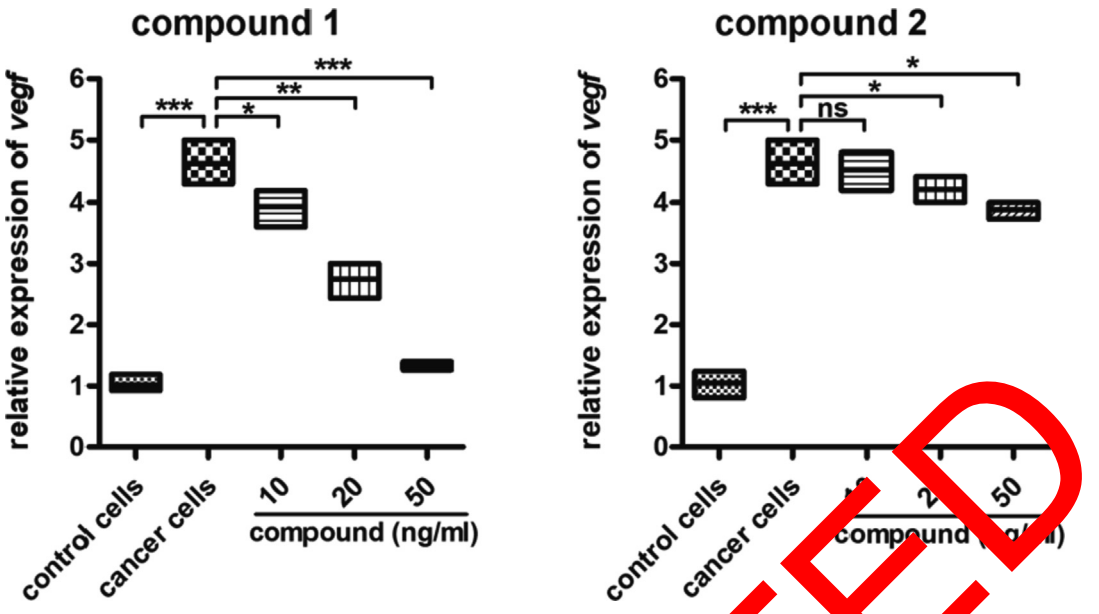

Fig. 6 Regulated VEGF signaling pathway signaling pathway in the pancreatic cancer cells of PC-1 after treated with the above compound. In logical growth, the pancreatic cancer cells of PC-1 were gathered and inoculated into the plate of cell culture, the treatment was subsequently finished with the above compounds at various concentrations. The real time RT-PCR was utilized to detect the VEGF signaling pathway in the pancreatic cancer cells of PC-1. * means $P < 0.05$, ** means $P < 0.01$ and *** means $P < 0.005$.

3.3. Compound significantly reduce the viability of the PC-1 pancreatic cancer cells

After designing and creating the compounds having novel structures, the treatment activity of above compounds against the PC-1 pancreatic cancer cells viability was determined firstly. Thus, the assay of CCK-8 was performed in this paper, and thePC-1 pancreatic cancer cells viability was measured. As we can know from the Fig. 4, the control group had a higher viability level for the pancreatic cancer cells of PC-1. After treating through the **1**, the viability of the pancreatic cancer cells of PC-1 was down-regulated remarkably, which is evidently different from control group. The suppression of this compound was even much more powerful than that in 5-Fu, the positive control drug. Nevertheless, the **2** only exhibited slight effect against the viability of the pancreatic cancer cells of PC-1.

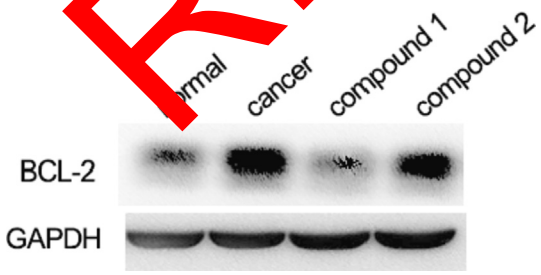

Fig. 7 Obviously down-regulated expression of BCL-2 in the PC-1 pancreatic cancer cells after the treatment of compound. The pancreatic cancer cells of PC-1 were gathered and treated by compound with serial different concentrations. The BCL-2 in the PC-1 pancreatic cancer cells was measured with western blotting assay.

3.4. Compound reduced the migration and viability of the PC-1 pancreatic cancer cells

In the previous study, we have demonstrated that the **1** could decrease the viability of the pancreatic cancer cells of PC-1, which is much motor powerful than that of **2**. Moreover, the compounds' effect against the invasion and migration of the pancreatic cancer cells of PC-1 was still required to be in-depth studied. The outcomes in Fig. 5 suggested that in contrast to control cancer cells, the **1** could significantly decrease the invasion and migration of cancer cells. Nevertheless, after treating through **2**, there exist only slight effect on the viability and migration of the pancreatic cancer cells of PC-1.

3.5. Compound showed excellent regulatory effect on the VEGF signaling pathway in the PC-1 pancreatic cancer cells

As we demonstrated in the earlier research, the new compound showed outstanding inhibitory activity against the invasion, migration and viability of the pancreatic cancer cells of PC-1. As formerly reported, the VEGF signaling pathway in the pancreatic cancer cells of PC-1 possesses an essential effect in developing the pancreatic cancer. As a result, the real time RT-PCR was in-depth performed and the VEGF signaling pathway activation in the pancreatic cancer cells of PC-1 was tested. The outcomes in Fig. 6 exhibited that in comparison with control group, there exist a markedly down-regulated VEGF signaling pathway level in the pancreatic cancer cells of PC-1. There was significantly difference between the above groups. Under treating with our novel compound, the VEGF signaling pathway relative expression in the pancreatic cancer cells of PC-1 was down-regulated markedly, which is much more outstanding than the **2**.

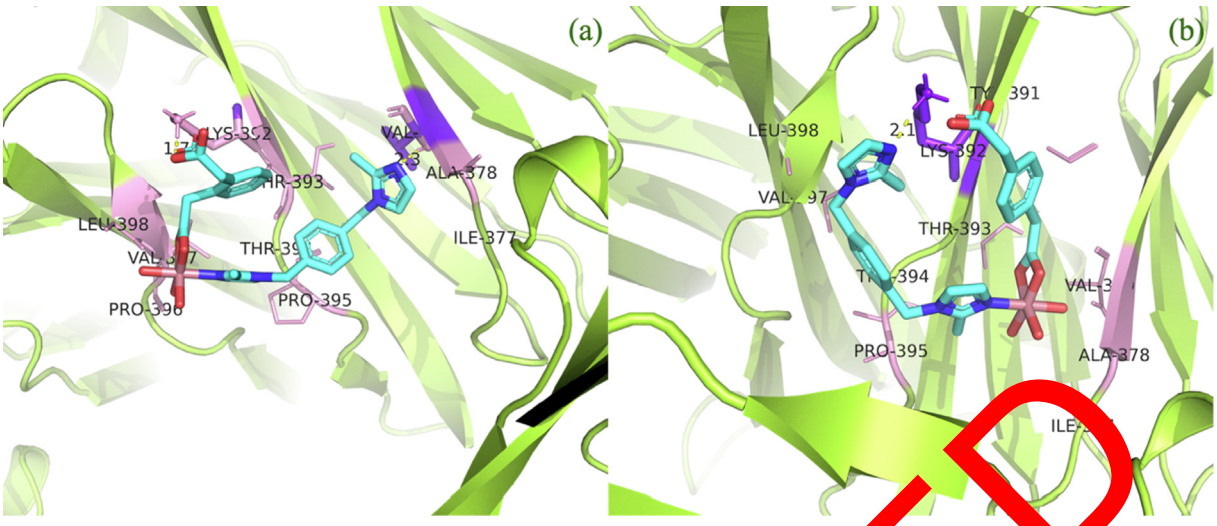

Fig. 8 Binding conformations of complex 1 (a) and complex 2 (b), their binding affinity energies are −7.0 and −6.84 kcal/mol, respectively. The active residues are colored as purple, and the binding interactions are shown as dotted lines.

3.6. Compound obviously reduced the expression of BCL-2 in the PC-1 pancreatic cancer cells

In the previous study, we have demonstrated that the compound exhibited superb treatment activity against the PC-1 pancreatic cancer cells via suppressing the cancer cells migration and viability, as well the VEGF signaling pathway activation. As the BCL-2 was the bio-maker of the cell apoptosis, furthermore, whether the compound could also influence the activation of the apoptotic signaling pathway was explored in our work. On the basis of Fig. 7, in contrast to normal cancer cells, the BCL-2 in the cancer cells was much higher than that in the control normal cells. Nevertheless, the exposure of compound **1** could significantly decrease the BCL-2 expression in the cancer cells, which is also more efficient than the biological activity of compound **2**.

3.7. Molecular docking

Vascular endothelial growth factor (VEGF) is promised specific domain-containing receptor and exhibits excellent biological activity (Raja et al., 2012). The regulation of VEGF protein is strong signaling probe of antitumor drug targets, thus, the two Co complexes have been studied by molecular docking simulation with 5 K65 receptor protein for investigating their potential anti-cancer activity. As described in the aforementioned section, for each of the Co complex, 50 possible binding poses have been evaluated. The binding conformations that with the lowest binding affinity energies for complexes **1** and **2** are shown in Fig. 8. Explicitly, the binding affinity energies are −7.0 and −6.84 kcal/mol, respectively.

The difference of the binding affinity energies is only about 0.1 kcal/mol, which is hard to distinguish which complex is more preferable for binding with the target probe from the energetical point of view. However, when look into the details of the binding conformation, we can see that complex **1** has formed two binding interactions (Fig. 8a), the carboxyl group is interacting with active residue LYS-392 (1.7 Å) and the imidazole is interacting with active residue VAL-379 (2.3 Å). In contrast, complex **2** is only formed one binding interaction with active residue LYS-392 (2.1 Å), as can be seen from Fig. 8b. Thus, we can conclude that complex **1** has higher activity in comparison to complex **2**, although their binding affinity energies are almost identical. The above results suggest that the *ortho*-position structure is more preferable when binding to the given target protein and shed light on future anti-cancer drug design.

4. Conclusion

In conclusion, we have created two Co(II) CPs from 1,4-bis(2-methylimidazol-1-ylmethyl)benzene, a semi-rigid ligand with different carboxylic acid co-ligandsand Co(II) nitrate salts. The assay of CCK-8 revealed that complex **1** was more superior to complex **2** on suppressing the viability of cancer cell. The detection of trans-well subsequently exhibited that complex **1** markedly decreased the invasion and migration of pancreatic cancer cells, in comparison with complex **2**. Then, the VEGF signaling pathway activation was evidently down-regulated via complex **1**, but not by complex **2**. Finally, we proved that the expression level of the BCL-2 protein was reduced by complex **1**, suggested complex **1**'s promotion effect against the apoptosis of cancer cell. Thus, we confirmed that complex **1** was much superior to complex **2** on treating pancreatic cancer via suppressing the cancer cell invasion, migration and viability ability.

Data availability

The IR spectra of complexes **1**–**2** (Fig. S1); Bond lengths for **1** (Table S1); Bond angles for **1** (Table S2); Bond lengths for **2** (Table S3); Bond angles for **2** (Table S4); the information could be found in the supporting information file.

Declaration of Competing Interest

The authors declare that they have no known competing financial interests or personal relationships that could have appeared to influence the work reported in this paper.

Acknowledgments

Not applicable.

Funding

The research was supported by the Research Fund for Hepatobiliary and Pancreatic Malignancies of Hubei Chen Xiaoping Science and Technology Development Foundation (Youth Fund) (CXPJJH11900001-2019341).

Appendix A. Supplementary data

Supplementary data to this article can be found online at https://doi.org/10.1016/j.arabjc.2021.103572.

References

Abedi, M., Mahmoudi, G., Hayati, P., Machura, B., Zubkov, F.I., Mohammadi, K., Bahrami, S., Derikvandi, H., Mehrabadi, Z., Kirillov, A.M., 2019. A 3D heterometallic Ni(ii)/K(i) MOF with a rare rna topology: synthesis, structural features, and photocatalytic dye degradation modeling. New J. Chem. 43, 17457–17465.

Aghaee, M., Mohammadi, K., Hayati, P., Ahmadi, S., Yazdian, F., Gutierrez, A., Rouhani, S., Msagati, T.A.M., 2021. Morphology design and control of a novel 3D potassium metal-organic coordination polymer compound: Crystallography, DFT, thermal, and biological studies. J. Mol. Struct. 1228, 129434.

Ansari, D., Tingstedt, B., Andersson, B., Holmquist, F., Sturesson, C., Williamsson, C., Sasor, A., Borg, D., Bauden, M., Andersson, 2016. Pancreatic cancer: yesterday, today and tomorrow. Futu Oncol. 12, 1929–1946.

Bear, A.S., Vonderheide, R.H., O'Hara, M.H., 2020. C es and Opportunities for Pancreatic Cancer Immunother y. Ca r Cell 38, 788–802.

Dutta, A., Pan, Y., Liu, J., Kumar, A., 202 Multi p isoreticular metal-organic frameworks: P ciple rent status and challenges. Coord. Chem. Rev. 4 214074.

Jagadeesan, S., Balasubramanian, V. th n, P., Neub er, M., Häussinger, D., Palivan, C.G., 20 3. Wate oluble Co(III) Complexes of Substituted Phena rolines with l Selective Anticancer Activity. Inorg. Ch . 52, 12535–12544.

Karadagi, A., Cavedon, A , Zemach I., Nowak, G., Eybye, M.E., Zhu, X., Guadagnin, E. White A.A., Rice L.M., Frassetto, A.L., Strom, S., Jorns, C., Ma P.G.V., s, E., 2020. Systemic modified mess ger NA fo replacement therapy in alpha 1-antitrypsin ficiency. ci. Rep. 052.

Lei, B., W M., ng Z., Qi, W., Su, R., He, Z., 2018. Constructin R ox-Respo ve Metal-Organic Framework Nanocarriers f Anticancer Drug Delivery. ACS Appl. Mater. Interfaces 10, 160 16706.

Liu, W., Yan, Q., Xia, Wang, X., Kumar, A., Wang, Y., Liu, Y., Pan, Y., Liu, J., 2021. Recent advances in cell membrane coated metal–organic frameworks (MOFs) for tumor therapy. J. Mater. Chem. B 9, 4459–4474.

Liu, W., Pan, Y., Zhong, Y., Li, B., Ding, Q., Xu, H., Qiu, Y., Ren, F., Li, B., Muddassir, M., Liu, J., 2021. A multifunctional aminated UiO-67 metal-organic framework for enhancing antitumor cytotoxicity through bimodal drug delivery. Chem. Eng. J. 412, 127899.

Lobner, E., Humm, A.S., Mlynek, G., Kubinger, K., Kitzmüller, M., Traxlmayr, M.W., Djinović-Carugo, K., Obinger, C., 2017. Two-faced Fcab prevents polymerization with VEGF and reveals thermodynamics and the 2.15 Å crystal structure of the complex. MAbs 9, 1088–1104.

Pan, Y., Luo, Z., Wang, X., Chen, Q., Chen, J., Guan, Y., Liu, D., Xu, H., Liu, J., 2020. A versatile and multifunctional metal–organic framework nanocomposite toward chemo-photodynamic therapy. Dalt. Trans. 49, 5291–5301.

Pepió, B., Contreras-Pereda, N., Su z-Garc S., Hayati, P., Benmansour, S., Retailleau, P., orsali, A., z-Molina, D., 2021. Solvent-tuned ultrasonic s thesis of 2 coordination polymer nanostructures a flakes. Ultrason. nochem. 72, 105425.

Raja, D.S., Bhuvanesh, S.P., N rajan, 2012. novel water soluble ligand bridge obalt(coordination polymer of 2-oxo-1,2-dihydroquin e-3-c ehyde nicotinic) hydrazone: evaluation o he DNA ding, rotein interaction, radical scavengin d nticancer acti Dalt. Trans. 41, 4365–4377.

Rashidi, N., ard, M S., Hayati, P., Janczak, J., Yazdian, F., 2020. Green approach for rication of a novel Zn(II) supramolecular c pound as new prec r to produce nano-sized Zinc(II) oxide: rystallography, topology, Hirshfeld Surface Analysis and biological activities. Mol. Struct. 1208, 127885.

Sh rick, G.M., 15. Crystal structure refinement with SHELXL. Crystall Sect. C Struct. Chem. 71, 3–8.

Souri, P., Rezvani, A.R., Janczak, J., 2018. The effects of modifying reaction conditions in green sonochemical synthesis of a c p (II) coordination polymer as well as in achieving to different morphologies of copper(II) oxide micro crystals via solid-state process. Inorg. Chim. Acta 483, 516–526.

Sukanya, P., Reddy, C.V.R., 2018. Synthesis, characterization and in vitro anticancer, DNA binding and cleavage studies of Mn (II), Co (II), Ni (II) and Cu (II) complexes of Schiff base ligand 3-(2-(1-(1H-benzimidazol-2-yl)ethylidene)hydrazinyl)quinoxalin-2(1H)-one and crystal structure. Appl. Organomet. Chem. 32, e4526.

Tempero, M.A., 2019. Guidelines Updates: Pancreatic Cancer. J. Natl. Compr. Canc. Netw. 17, 603–605.

Wang, N., Feng, Y.C., Shi, W., Zhao, B., Cheng, P., Liao, D.Z., Yan, S.P., 2012. Synthesis, structure, fluorescent and magnetic properties of a series of coordination polymers based on a long and flexible bis-triazole ligand. CrystEngComm 14, 2769–2778.

Zhang, H.R., Meng, T., Liu, Y.C., Chen, Z.F., Liu, Y.N., Liang, H., 2016. Synthesis, characterization and biological evaluation of a cobalt(II) complex with 5-chloro-8-hydroxyquinoline as anticancer agent. Appl. Organomet. Chem. 30, 740–747.

Zhong, Y., Li, X., Chen, J., Wang, X., Wei, L., Fang, L., Kumar, A., Zhuang, S., Liu, J., 2020. Recent advances in MOF-based nanoplatforms generating reactive species for chemodynamic therapy. Dalt. Trans. 49, 11045–11058.